Desalination and Water Treatment
www.deswater.com
doi: 10.5004/dwt.2021.27484

231 (2021) 27–43
August

Study on effect of dissimilarity of mass flow rate on energy metrics of solar energy-based double slope water purifier by incorporating N alike PVT compound parabolic concentrator collectors

Desh Bandhu Singh[a,*], Rakesh Kumar Yadav[b], Yatender Chaturvedi[c], Mukesh Kumar[d], Gaurav Kumar Sharma[e], Navneet Kumar[f]

[a]*Department of Mechanical Engineering, Graphic Era Deemed to be University, Bell Road, Clement Town, Dehradun – 201306, Uttarakhand, India, email: dbsiit76@gmail.com/deshbandhusingh.me@geu.ac.in*
[b]*Motherhood University, Roorkee, Haridwar, Uttarakhand, India – 247661, email: er.rakeshyadava@gmail.com*
[c]*Sunder Deep Group of Institutions, Ghaziabad, UP, India, email: yatender.neeru@gmail.com*
[d]*Department of Mechanical Engineering, IEC College of Engineering and Technology, Greater Noida – 201306, G.B. Nagar, Uttar Pradesh, India, email: drmukeshkumar.me@gmail.com*
[e]*Department of Mechanical Engineering, College of Engineering and Technology, IILM Academy of Higher Education, Greater Noida – 201306, G.B. Nagar, Uttar Pradesh, India, email: kavi.me.siet@gmail.com*
[f]*Galgotias College of Engineering and Technology, Greater Noida – 201306, G.B. Nagar, Uttar Pradesh, India, email: navneet.kumar@galgotiacollege.edu*

Received 20 September 2020; Accepted 2 June 2021

ABSTRACT

This work focuses on the effect of dissimilarity of mass flow rate ($\dot{m}_f$) on energy metrics of double slope (DS) solar energy-based water purifier (SEBWP) by incorporating N equal partially covered photovoltaic thermal (PVT) compound parabolic concentrating collectors (NPVT-CPCs) having series connection keeping water depth as 0.14 m. All four kinds of weather conditions for New Delhi have been taken for the computation of different parameters. The equations obtained for different parameters after solving energy balance equations for all components of the proposed system have been fed to mathematical programming done in MATLAB for computing different parameters. The computation of different relevant parameters has been performed for various values of $\dot{m}_f$ while keeping N as constant to know the effect of dissimilarity of $\dot{m}_f$ on the energy metrics for DS type SEBWP in active mode. It has been concluded that the value of energy payback time for DS type SEBWP in active mode enhances, but life cycle conversion efficiency (LCCE) for the system diminishes with the enhancement in the value of $\dot{m}_f$ at a given value of water depth of 0.14 m. Values of LCCE taking energy and exergy as a basis have been found to be constant beyond $\dot{m}_f$ values of 0.10 and 0.11 kg/s respectively.

Keywords: Energy metrics; Mass flow rate; N; Double slope solar still

1. Introduction

Energy and fresh water are two basic needs for the survival of life on the planet earth. However, energy and fresh water are not available in abundance to meet the need of human beings as the globe is facing the scarcity of both these basic items. The conventional source of energy is detrimental to the environment due to the emission of

* Corresponding author.

1944-3994/1944-3986 © 2021 Desalination Publications. All rights reserved.

greenhouse gases and hence to human beings and the source of conventional energy is limited, too. The solar energy technology-based systems which are simple and environment friendly have the potential to meet both energies as well as fresh water needs. The solar energy-based water purifier (SEBWP) in active mode involving solar panels can generate DC electric power as well as fresh water. This type of solar energy-based system is self-sustainable and hence can be installed and operated successfully at remote locations where sunlight is present in abundance. Energy metrics analysis of the solar energy-based system is essential because it tells whether the system is technically feasible from energy and exergy viewpoints.

The active type SEBWP came into existence in 1983 [1] and from that time, many new designs have been reported by various researchers around the globe. The active type SEBWP means the provision of an external source of heat to the basin of passive-type SEBWP. The external source of heat can be made available as solar collectors/industry waste heat using a heat exchanger or similar other kinds of provision can be made. Rai and Tiwari [1] reported the enhancement in yield of active type SEBWP by incorporating one conventional flat plate collector (FPC) over passive type SEBWP of the same basin area due to the addition of heat to the basin in an active mode of operation. This water purifier was not self-sustainable as the pump needed some electric power for working which was supplied through the grid.

The active type SEBWP in the forced mode of operation can be made self-sustainable by incorporating solar panels. Kumar and Tiwari [2] proposed the integration of photovoltaic thermal (PVT) with FPC for supplying heat to the basin of passive-type SEBWP taking inspiration from the work of Kern and Russell [3]. It was reported by Kern and Russell [3] that the electrical efficiency of the solar panel got increased upon integration of solar panels with solar collectors due to the removal of heat by the fluid passing below the panel. Kumar and Tiwari [2] reported the improvement in output by 3.5 times over the similar passive type SEBWP due to the addition of heat by two collectors in which only one of them was integrated with PVT for making the system self-sustainable. The work of Kumar and Tiwari [2] was extended by Singh et al. [4] for double slope (DS) type SEBWP in active mode. Further, Singh et al. [5] and Tiwari et al. [6] reported the experimental investigation of SEBWP by incorporating two FPCs in which both FPCs were partially integrated with PVT. They reported an enhancement in DC electrical output; however, the yield of fresh water was less as compared to the system reported by Kumar and Tiwari [2]. The heat gain was less because more area of FPCs was covered by PVT. Further, active type SEBWP was studied under an optimized situation [7–11]. It was reported that the DS type SEBWP under optimized conditions by incorporating N alike PVT-FPCs had 74.66% higher energy payback time (ENPBT) over passive type DS-SEBWP. The value of the exergoeconomic parameter for single slope type SEBWP was found to be 47.37% higher than the passive type single slope SEBWP of the same basin area. Sahota and Tiwari [12] reported the use of nanofluid in DS type SEBWP in active mode for enhancing the fresh water output. Carranza et al. [13] have experimentally investigated the performance of DS type SEBWP loaded with nanofluid by incorporating preheating of saline water and concluded that water yield increases due to better thermophysical properties of nanofluid as compared to the base fluid. Kouadri et al. [14] have investigated solar still by incorporating zinc and copper oxides for the location of Algeria and compared the yield with conventional SEBWP and concluded that the water yield was improved by 79.39% due to having the better thermophysical characteristic of nanofluid.

The output of SEBWP could further be enhanced by changing the design of the solar collector which could absorb a higher amount of heat from the sun or by changing the design of solar still. PVT integrated FPC could gain higher heat if some concentrating part was integrated with FPC. With this concept in mind, Atheaya et al. [15] proposed a PVT integrated compound parabolic concentrator collector (CPC) and reported its thermal model which was further extended by Tripathi et al. [16] for N collectors connected in series and loop was opened. Singh and Tiwari [17–19], Gupta et al. [20,21], Singh et al. [22,23] and Sharma et al. [24] investigated SEBWP of basin type by incorporating characteristic equations development and concluded that SEBWP of double slope type performs better than SEBWP of single slope type under optimized conditions of mass flow rate and a number of collectors at 0.14 m water depth due to better distribution of solar energy in the case of double slope type. Prasad et al. [25], Bharti et al. [26], Singh [27] investigated SEBWP of double slope type from a sensitivity viewpoint and concluded that the sensitivity analysis helps designer and installer of solar systems as which parameter should be focused more for a particular application.

The heat gain by the solar collector can be enhanced by providing evacuated tubes because convection loss does not take place through a vacuum. Sampathkumar et al. [28] investigated the SEBWP by incorporating an evacuated tubular collector and reported an increase of 129% over the SEBWP of the same basin area due to the addition of heat to the basin by collectors. An investigation of SEBWP in the natural mode of operation by incorporating evacuated tubes was done by Singh et al. [29] and reported exergy efficiency lying in the range of 0.15% to 8%. Further, an investigation of SEBWP incorporated with evacuated tubes was done in the forced mode of operation by inserting pump between collector and basin and reported enhanced fresh water output as compared to the similar system operated in natural mode due to better circulation of fluid in the forced mode of operation [30]. Mishra et al. [31] reported characteristic equation development for N alike series-connected evacuated tubular collector (ETC). The work reported by Mishra et al. [31] was further extended by Singh et al. [32–34]. The thermal modeling of basin type SEBWP by incorporating N alike ETCs was reported by them and comparison was also made between single slope active water purifier and DS type SEBWP in active mode taking energy, exergy, energy metrics, exergoeconomic and enviroeconomic parameters as a basis. Issa and Chang [35] further extended the work of Singh et al. by connecting ETCs in a mixed mode of operation experimentally and reported enhanced output as compared to a similar setup in passive mode due to heat addition by collectors in active mode. Moreover, Singh and Al-Helal [36], Singh [37] and Sharma et al. [38,39]

reported the development of characteristic equations and the observations based on the energy metrics for SEBWP by incorporating evacuated tubular collector as well as compound parabolic concentrator integrated evacuated tubular collector.

Patel et al. [40–42] have reviewed SEBWP recently by incorporating different types of collectors. Further, Singh et al. [43] reviewed SEBWP by incorporating different types of collectors and loaded with nanofluid with an aim to find the effect of nanofluid on the performance of active SEBWP. Nanofluid is obtained by mixing a small amount of nanoparticles into water. The effect of adding nanoparticles to water in SEBWP is to increase the output (potable water and exergy) of SEBWP. The better performance of nanofluid-loaded SEBWP than loaded with water is due to the possession of better thermo-physical characteristics of nanofluid as compared to water. Bansal et al. [44] have reported the mini-review of changing the material of absorber on the performance of solar still. Shankar et al. [45] have studied ETC integrated SEBWP in natural as well forced mode and concluded that forced mode is better for the environment as higher carbon credit was observed in forced mode due to more addition of heat to the basin in the case of forced mode. Abdallah et al. [46] have investigated spherical and pyramid basin SEBWP and concluded that the spherical basin SEBWP gave 57.1% higher water yield due to better utilization of solar radiation in the case of the spherical basin.

From the current literature survey, it is seen that the effect of mass flow rate ($\dot{m}_f$) on the energy metrics of DS type SEBWP by incorporating N alike PVT-CPCs has not been reported by any researchers throughout the globe. The difference between the earlier reported work and the proposed work lies in the fact that energy metrics of active type SEBWP was computed at a fixed value of $\dot{m}_f$ and N; whereas, in the proposed work, energy metrics of DS type SEBWP in active mode has been computed by varying values of $\dot{m}_f$ and it has been tried to find the optimum values of $\dot{m}_f$ taking energy metrics as a basis.

2. System metaphors

DS type SEBWP by incorporating N alike partly covered PVT-CPCs shaving series connection has been shown in Fig. 1. The specification of system has been revealed as Table 1. In the proposed SEBWP, heat is provided by N equal partially covered PVT-CPCs and hence works in active mode. When sunlight falls on the surface of condensing cover, it is transmitted to the water surface after reflection and absorption. The transmissivity of the glass is about 0.95. So, a major portion of sunlight is transmitted to the water surface. Again, after reflection and absorption by the water surface, the sunlight is transmitted to the blackened surface kept at the bottom of the basin where almost all parts of radiation get absorbed. The temperature of the blackened surface kept at the bottom rises and heat is transferred to water from the blackened surface. Water in the basin also receives heat from N alike series-connected collectors. Thus the temperature of water rises and evaporation occurs which depends on the temperature difference between the water surface and the inside surface of the glass cover. The vapor gets condensed through film-wise condensation at the inside surface of the glass. The condensed water trickles down under gravity and gets collected at the channel fixed at the lower side. The fresh water is then collected in a jar through a tube connected to the channel.

3. Mathematical modeling based on energy balance equations

Mathematical modeling of N equal partially covered PVT-CPCs integrated to DS type SEBWP means writing equations for all its components by equating input energy to output energy. Following assumptions presented in Singh and Tiwari [17–19], the mathematical modeling can be done as follows:

3.1. Heat gain for N equal partially covered PVT-CPCs

The heat gain from N equal partially covered PVT-CPCs and temperature at the outlet of the last collector can be written as follows [15,16]:

$$\dot{Q}_{\mathrm{uN}} = \frac{\left(1-K_k^N\right)}{\left(1-K_k\right)}\left(AR_R\left(\alpha\tau\right)\right)_1 I_b\left(t\right) + \frac{\left(1-K_k^N\right)}{\left(1-K_k\right)}\left(AF_RU_L\right)_1\left(T_{\mathrm{fi}}-T_a\right) \quad (1)$$

$$T_{\mathrm{foN}} = \frac{I_b\left(t\right)\left(AR_R\left(\alpha\tau\right)\right)_1}{\dot{m}_fC_f}\frac{\left(1-K_k^N\right)}{\left(1-K_k\right)} + \frac{T_a\left(AF_RU_L\right)_1}{\dot{m}_fC_f}\frac{\left(1-K_k^N\right)}{\left(1-K_k\right)} + T_{\mathrm{fi}}K_k^N \quad (2)$$

Here, $T_{\mathrm{fi}} = T_w$. NPVT-CPCs are in a closed-loop in the proposed water purifier as the fluid at the outlet of the last collector is allowed to flow to the basin of solar still. Hence, $T_{\mathrm{wo}} = T_{\mathrm{foN}}$.

The electrical efficiency of solar cells (η_{cN}) of NPVT-CPCs can be expressed as [47,48]:

$$\eta_{\mathrm{cN}} = \eta_o\left[1-\beta_o\left(\overline{T}_{\mathrm{cN}}-T_o\right)\right] \quad (3)$$

Here, η_o stands for efficiency under standard state test conditions and $\overline{T}_{\mathrm{cN}}$ stands for the average value of the temperature of the solar cell of NPVT-CPCs.

3.2. Mathematical equation based on equating input and output energies for DS type SEBWP in active mode

The fundamental equations for different components of DS type SEBWP in active mode taking balancing energy as a basis can be written as follows:

3.2.1. For the inside surface of glass cover facing east

$$\alpha_g' I_{\mathrm{SE}}\left(t\right)A_{\mathrm{gE}} + h_{\mathrm{1wE}}\left(T_w-T_{\mathrm{giE}}\right)\frac{A_b}{2} - h_{\mathrm{EW}}\left(T_{\mathrm{giE}}-T_{\mathrm{giW}}\right)$$

$$A_{\mathrm{gE}} = \frac{K_g}{L_g}\left(T_{\mathrm{giE}}-T_{\mathrm{goE}}\right)A_{\mathrm{gE}} \quad (4)$$

where $h_{\mathrm{1wE}} = h_{\mathrm{rwgE}} + h_{\mathrm{cwgE}} + h_{\mathrm{ewgE}}$ which is called net heat transfer coefficient (NHTC) from the surface of the water to the

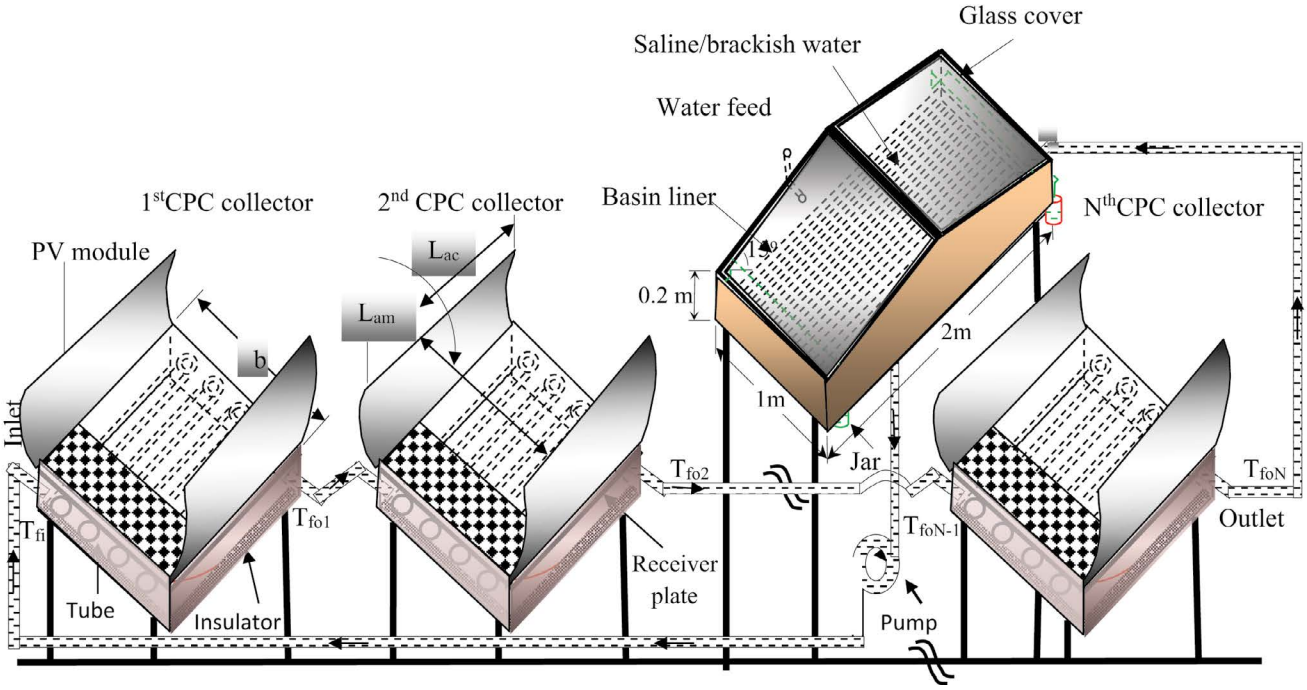

Fig. 1. Schematic diagram of DS type SEBWP integrated with N equal partially covered PVT-CPCs having a series connection.

inside surface of the glass cover and α_g' represents the fraction of solar flux absorbed by the glass cover.

3.2.2. For outside surface of glass cover facing east

$$\frac{K_g}{L_g}\left(T_{\mathrm{giE}}-T_{\mathrm{goE}}\right)A_{\mathrm{gE}}=h_{1\mathrm{gE}}\left(T_{\mathrm{goE}}-T_a\right)A_{\mathrm{gE}} \tag{5}$$

where $h_{1\mathrm{gE}}=h_{\mathrm{rgE}}+h_{\mathrm{cgE}}$ or $h_{1\mathrm{gE}}=5.7+3.8$ V.

3.2.3. For the inside surface of glass cover facing west

$$\alpha_g' I_{\mathrm{SW}}\left(t\right)A_{\mathrm{gW}}+h_{1\mathrm{wW}}\left(T_w-T_{\mathrm{giW}}\right)\frac{A_b}{2}+h_{\mathrm{EW}}\left(T_{\mathrm{giE}}-T_{\mathrm{giW}}\right)$$
$$A_{\mathrm{gE}}=\frac{K_g}{L_g}\left(T_{\mathrm{giW}}-T_{\mathrm{goW}}\right)A_{\mathrm{gW}} \tag{6}$$

where $h_{1\mathrm{wW}}=h_{\mathrm{rwgW}}+h_{\mathrm{cwgW}}+h_{\mathrm{ewgW}}$ which is called NHTC from the surface of the water to the inside surface of the glass cover which is oriented towards the east.

3.2.4. For outside surface of glass cover facing west

$$\frac{K_g}{L_g}\left(T_{\mathrm{giW}}-T_{\mathrm{goW}}\right)A_{\mathrm{gW}}=h_{1\mathrm{gW}}\left(T_{\mathrm{goW}}-T_a\right)A_{\mathrm{gW}} \tag{7}$$

where $h_{1\mathrm{gW}}=h_{\mathrm{rgW}}+h_{\mathrm{cgW}}$ or $h_{1\mathrm{gW}}=5.7+3.8$ V.

3.2.5. For blackened surface placed at the bottom of the basin

$$\alpha_b'\left(I_{\mathrm{SE}}\left(t\right)+I_{\mathrm{SW}}\left(t\right)\right)\frac{A_b}{2}=h_{\mathrm{bw}}\left(T_b-T_w\right)A_b+h_{\mathrm{ba}}\left(T_b-T_a\right)A_b \tag{8}$$

where α_b' is the fraction of solar flux absorbed by the basin liner.

3.2.6. For water mass in the basin

$$\left(M_wC_w\right)\frac{dT_w}{dt}=\left(I_{\mathrm{SE}}\left(t\right)+I_{\mathrm{SW}}\left(t\right)\right)\alpha_w'\frac{A_b}{2}+h_{\mathrm{bw}}\left(T_b-T_w\right)$$
$$A_b-h_{1w}\left(T_w-T_{\mathrm{giE}}\right)\frac{A_b}{2}-h_{1w}\left(T_w-T_{\mathrm{giE}}\right)\frac{A_b}{2}+\dot{Q}_{\mathrm{uN}} \tag{9}$$

On the simplification of Eq. (1) and Eqs. (4)–(9) using mathematical concept and proper arrangement of various terms, one can obtain the expression for the temperature of the water as:

$$T_w=\frac{\bar{f}_1\left(t\right)}{a_1}\left(1-e^{-a_1t}\right)+T_{w0}e^{-a_1t} \tag{10}$$

After finding the value of T_w from Eq. (10), one can proceed to obtain glass temperature for NPVT-CPC-SEBDSWP (SEBDSWP – solar energy based double slope water purifier) as follows.

$$T_{\mathrm{giE}}=\frac{A_1+A_2T_w}{P} \tag{11}$$

$$T_{\mathrm{giW}}=\frac{B_1+B_2T_w}{P} \tag{12}$$

$$T_{\mathrm{goE}}=\frac{\frac{K_g}{L_g}T_{\mathrm{giE}}+h_{1\mathrm{gE}}T_a}{\frac{K_g}{L_g}+h_{1\mathrm{gE}}} \tag{13}$$

$$T_{\mathrm{goW}} = \frac{\frac{K_g}{L_g} T_{\mathrm{giW}} + h_{1\mathrm{gW}} T_a}{\frac{K_g}{L_g} + h_{1\mathrm{gW}}} \tag{14}$$

The different unknown terms in Eqs. (1)–(14) are given in Appendix-A. The fresh water output from NPVT-CPC-SEBDSWP can be written as:

$$\dot{m}_{\mathrm{ew}} = \left[\frac{h_{\mathrm{ewE}} \frac{A_b}{2} \left(T_w - T_{\mathrm{giE}} \right) + h_{\mathrm{ewW}} \frac{A_b}{2} \left(T_w - T_{\mathrm{giW}} \right)}{L} \right] \times 3{,}600 \tag{15}$$

4. Experimental validation of solar energy-based double slope water purifier by incorporating N alike PVT compound parabolic concentrator collectors

4.1. For N alike PVT compound parabolic concentrator collectors

If receiver area is made equal to module area, that is, $A_{\mathrm{rm}} = A_{\mathrm{rc}}$, N alike partially covered PVT compound parabolic concentrator collectors becomes N alike fully covered PVT compound parabolic concentrator collectors. The experimental validation of fully covered PVT compound parabolic concentrator collectors has been done by Tripathi and Tiwari [49]. They validated N alike fully covered PVT compound parabolic concentrator collectors taking values of N, mass flow rate, packing factor and concentration ratio as 1, 0.01 kg/s, 0.89, and 2, respectively. The collection of data was done from 9:00 to 16:00 h on September 21 and 22, 2015 for solar intensity, ambient air temperature, tank temperature, cell temperature, and temperature-dependent electrical efficiency. The statistical analysis was carried out and they found the value of coefficient of correlation between theoretical and experimental values as 0.98 for water temperature which represents a fair agreement between theoretical and experimental values.

4.2. For solar energy-based double slope water purifier

The experimental validation of solar energy-based double slope water purifier has been carried out by Dwivedi and Tiwari [50] for New Delhi climatic conditions at different water depths taking basin area as 2 m^2. They have collected data for solar intensity, ambient air temperature, water temperature, condensing cover temperatures, and hourly yield for October 2005–September 2006. They evaluated heat transfer coefficients and hourly yield for April 2006 using various models namely Kumar and Tiwari [51], Dunkle [52], Adhikari et al. [53], Zheng et al. [54], and Clark [55]. They obtained the best result for heat transfer coefficient and hourly yield using Dunkle's model. A fair agreement was found between experimental and theoretical values of hourly yield using Dunkle's model taking percentage error as the basis.

5. Analysis

For the analysis of the effect of $\dot{m}_f$ for given N on the energy metrics of DS type SEBWP in active mode, 4 climatic situations for each month of the year have been taken. These climatic situations can be defined by a number of sunshine hours (N') and daily diffuse to daily global irradiation ratio (r') as follows [56].

- Clear day (blue sky) $r' \le 0.25$ and $N' \ge 9$ h
- Hazy day (fully) $0.25 \le r' \le 0.50$ and $7 \text{ h} \le N' \le 9$ h
- Hazy and cloudy (partially) $0.50 \le r' \le 0.75$ and $5 \text{ h} \le N' \le 7$ h
- Cloudy day (fully) $r' \ge 0.75$ and $N' \le 5$ h

5.1. Energy analysis

The expression of overall annual energy (E_{out}) for DS type SEBWP in active mode considering 1st law of thermodynamics can be expressed as:

$$E_{\mathrm{out}} = \frac{\left(M_{\mathrm{ew}} \times L \right)}{3{,}600} + \frac{\left(P_m - P_u \right)}{0.38} \tag{16}$$

where M_{ew} is annual potable water output obtained from DS type SEBWP in active mode, P_m is yearly electrical power received from PVT, P_u is yearly electrical power utilized by pump and L is latent heat. Here, factor 0.38 which is present in the denominator converts electrical energy (high-grade energy) into heat (low-grade energy). This factor is basically the efficacy of power output taken from conventional power plants [57].

The hourly electrical energy ($\dot{\mathrm{E}}\mathrm{x}_e$) for the solar panel used in DS type SEBWP in active mode can be expressed as follows:

$$\dot{\mathrm{E}}\mathrm{x}_e = A_m I_b(t) \sum_{1}^{N} \left(\alpha \tau_g \eta_{\mathrm{cN}} \right) \tag{17}$$

Eq. (17) can be used for evaluating daily electrical exergy of type (a) climatic situation by summing the hourly value of 10 h because the solar flux exists for 10 h only. A similar approach has been used to work out the daily electrical energy for rest types of climatic situation, that is, type (b) to type (d). The value of electrical energy on monthly basis for type (a) climatic situation has been evaluated as the multiplication of electrical energy on daily basis and the corresponding value of a number of clear days (n'). A similar approach has been used to work out the electrical energy on monthly basis for the rest types of climatic situations, that is, type (b) to type (d). The value of net electrical energy on monthly basis has been worked out by summing electrical energy values for type (a) to type (d) climatic situations. The value of electrical energy (P_m) on annual basis has been worked out by the summing of electrical energy on monthly basis for 12 months. A similar approach has been followed for the estimation of annual fresh water yield (M_{ew}).

5.2. Exergy analysis

Exergy analysis has been done on the basis of the 1st law (energy) and 2nd law (entropy) of thermodynamics. The hourly output thermal exergy $\dot{\mathrm{E}}\mathrm{x}_{\mathrm{out}}$ (W) for N-PVT-CPC-SEBDSWP can be expressed as [58]:

$$\dot{\mathrm{E}}\mathrm{x}_{\mathrm{out}} = h_{\mathrm{ewgE}} \times \frac{A_b}{2} \times \left[\left(T_w - T_{\mathrm{giE}} \right) - \left(T_a + 273 \right) \times \ln \left\{ \frac{\left(T_w + 273 \right)}{\left(T_{\mathrm{giE}} + 273 \right)} \right\} \right] + h_{\mathrm{ewgW}} \times \frac{A_b}{2} \times \left[\left(T_w - T_{\mathrm{giW}} \right) - \left(T_a + 273 \right) \times \ln \left\{ \frac{\left(T_w + 273 \right)}{\left(T_{\mathrm{giW}} + 273 \right)} \right\} \right] \tag{18}$$

where

$$h_{e,\mathrm{wg}} = 16.273 \times 10^{-3} h_{c,\mathrm{wg}} \left[\frac{P_w - P_{\mathrm{gi}}}{T_w - T_{\mathrm{gi}}} \right] \text{ [59]} \tag{19}$$

$$h_{c,\mathrm{wg}} = 0.884 \left[\left(T_w - T_{\mathrm{gi}} \right) + \frac{\left(P_w - P_{\mathrm{gi}} \right)\left(T_w + 273 \right)}{268.9 \times 10^3 - P_w} \right]^{\left(\frac{1}{3} \right)} \text{ [52]} \tag{20}$$

$$P_w = \exp\left[25.317 - \frac{5{,}144}{\left(T_w + 273 \right)} \right] \tag{21}$$

and

$$P_{\mathrm{gi}} = \exp\left[25.317 - \frac{5{,}144}{\left(T_{\mathrm{gi}} + 273 \right)} \right] \tag{22}$$

Eq. (18) can be used for evaluating daily thermal exergy of type (a) climatic situation by summing the hourly value of 10 h because the solar flux exists for 10 h only. A similar approach has been used to work out the daily thermal exergy for rest types of climatic situation, that is, type (b) to type (d). The value of thermal exergy on monthly basis for type (a) climatic situation has been evaluated as the multiplication of thermal exergy on daily basis and the corresponding value of number of clear days (*n'*). A similar approach has been used to work out the thermal exergy on monthly basis for rest types of climatic situations, that is, type (b) to type (d). The value of net thermal exergy on monthly basis has been worked out by summing thermal exergies values for type (a) to type (d) climatic situations. The value of thermal exergy on annual basis has been worked out by the summing of thermal energy on monthly basis for 12 months.

The value of yearly overall annual exergy gain ($G_{\mathrm{ex,annual}}$) for DS type SEBWP in active mode has been expressed as follows:

$$G_{\mathrm{ex,annual}} = \mathrm{Ex}_{\mathrm{out}} + \left(P_m - P_u \right) \tag{23}$$

5.3. Energy metrics

Energy metrics include energy payback time, energy production factor and life cycle conversion efficacy. The discussion of energy metrics for DS type SEBWP in active mode is important because it deals with the feasibility as well as the performance of the system. The energy payback time tells about the feasibility of DS type SEBWP in active mode from an energy viewpoint whereas life cycle conversion efficiency tells about the performance of the system taking energy as the basis.

5.3.1. Energy payback time

The time period needed to recover the total energy exhausted in preparing the materials (embodied energy) required for fabrication of NPVT-CPC-SEBDSWP is known as ENPBT. Following Tiwari and Mishra [60], it can be written as:

$$\text{ENPBT based on energy} = \frac{\text{Embodied energy } \left(E_{\mathrm{in}} \right)}{\text{Annual energy output } \left(E_{\mathrm{out}} \right)} \tag{24}$$

$$\text{ENPBT based on exergy} = \frac{\text{Embodied energy } \left(E_{\mathrm{in}} \right)}{\text{Annual exergy output } \left(G_{\mathrm{ex,annual}} \right)} \tag{25}$$

Here, embodied energy means the amount of energy used to manufacture the material required for DS type SEBWP integrated with N equal partially covered PVT-CPCs. The evaluation of embodied energy for DS type SEBWP integrated with N equal partially covered PVT-CPCs has been presented in Table 6.

5.3.2. Energy production factor

It gives the overall performance of the proposed DS type SEBWP integrated with N equal partially covered PVT-CPCs in forced mode and can be expressed as the ratio of energy/exergy output obtained from the system to embodied energy. Obviously, it is the opposite of ENPBT and ideal value on an annual basis is normally considered as unity. As per Tiwari and Mishra [60], energy production factor (ENPF) for NPVT-CPC-SEBDSWP on per year basis can be expressed as:

$$\text{ENPF based on energy} = \frac{E_{\mathrm{out}}}{E_{\mathrm{in}}} \tag{26}$$

$$\text{ENPF based on exergy} = \frac{G_{\mathrm{ex,annual}}}{E_{\mathrm{in}}} \tag{27}$$

Here, E_{out} is the overall energy output taking year as the basis at given values of $\dot{m}_f$ and N, E_{in} is embodied energy for DS type SEBWP integrated with N equal partially covered PVT-CPCs in forced mode at considered values of $\dot{m}_f$ and N and $G_{\mathrm{ex,annual}}$ is overall exergy output taking year as the basis at given values of $\dot{m}_f$ and N.

5.3.3. Life cycle conversion efficiency

It signifies the overall output of DS type SEBWP integrated with N equal partially covered PVT-CPCs in forced mode with regard to sunlight falling on the surface of DS type SEBWP integrated with N equal partially covered PVT-CPCs in forced mode for the life span of the system. The ideal value of life cycle conversion efficiency (LCCE) for DS type

SEBWP integrated with N equal partially covered PVT-CPCs in forced mode is considered as 1. The superior the assessment of LCCE, the system is considered superior. As per Tiwari and Mishra [60], LCCE for DS type SEBWP integrated with N equal partially covered PVT-CPCs in forced mode can be expressed as:

$$\text{LCCE based on energy} = \frac{E_{\text{out}} \times n - E_{\text{in}}}{E_{\text{sol}} \times n} \tag{28}$$

$$\text{LCCE based on exergy} = \frac{G_{\text{ex,annual}} \times n - E_{\text{in}}}{\left(\text{Annual solar exergy}\right) \times n} \tag{29}$$

Here E_{sol} is the value of sunlight falling on the surface of the system on yearly basis and n is the life span of system.

6. Methodology

The methodology to investigate the effect of $\dot{m}_f$ at given N on the energy metrics of DS type SEBWP integrated with N equal partially covered PVT-CPCs in forced mode are as follows:

Step I

Taking the value of solar flux on the horizontal plane from IMD located at Pune in India, the value of solar flux on the inclined plane has been evaluated using Liu and Jordan formula by the computational program in MATLAB. The data for surrounding temperature has been accessed from IMD situated at Pune in India.

Step II

The computation for potable water yielding per hour basis for different values of $\dot{m}_f$ at given N has been carried out with the help of Eq. (15) followed by the computation of potable water yielding on a per year basis.

Step III

The computation for exergy on the basis of per hour for different values of $\dot{m}_f$ at given N has been carried out with the help of Eqs. (17) and (18) followed by the calculation for exergy on per year basis.

Step IV

The calculation for gross energy output values at various values of $\dot{m}_f$ for given N has been performed using Eq. (16) followed by calculation for gross energy output on per year basis.

Step V

The calculation for gross exergy output values at various values of $\dot{m}_f$ for given N has been performed using Eq. (23) followed by calculation for gross exergy output on per year basis.

Table 1
Specifications of DS type SEBWP integrated with N equal partially covered PVT-CPCs

Component	Specification	Component	Specification
Double slope active solar still			
Length	2 m	Orientation	East-west
Width	1 m	Thickness of glass cover	0.004 m
Inclination of glass cover	15°	K_g	0.816 W/m-K
Height of smaller side	0.2 m	Thickness of insulation	0.1 m
Material of body	GRP	Thermal conductivity of insulation	0.166 W/m-K
Material of stand	GI	Cover material	Glass
PVT-CPC collector			
Type and no. of collectors	Tube in plate type, N	Aperture area	2 m^2
Receiver area of solar water collector	1.0 m × 1.0 m	Aperture area of module	0.5 m × 2.0 m
Collector plate thickness	0.002	Aperture area of receiver	0.75 m × 2.0 m
Thickness of copper tubes	0.00056 m	Receiver area of module	0.25 m × 1.0 m
Length of each copper tubes	1.0 m	Receiver area of collector	0.75 m × 1.0 m
K_i (Wm^{-1} K^{-1})	0.166	F'	0.968
FF	0.8	ρ	0.84
Thickness of insulation	0.1 m	τ_g	0.95
Angle of CPC with horizontal	30°	α_c	0.9
Thickness of toughen glass on CPC	0.004 m	β_c	0.89
Effective area of collector under glass	0.75 m^2	α_p	0.8
Pipe diameter	0.0125 m	Effective area of collector under PV module	0.25 m^2
DC motor rating	12 V, 24 W		

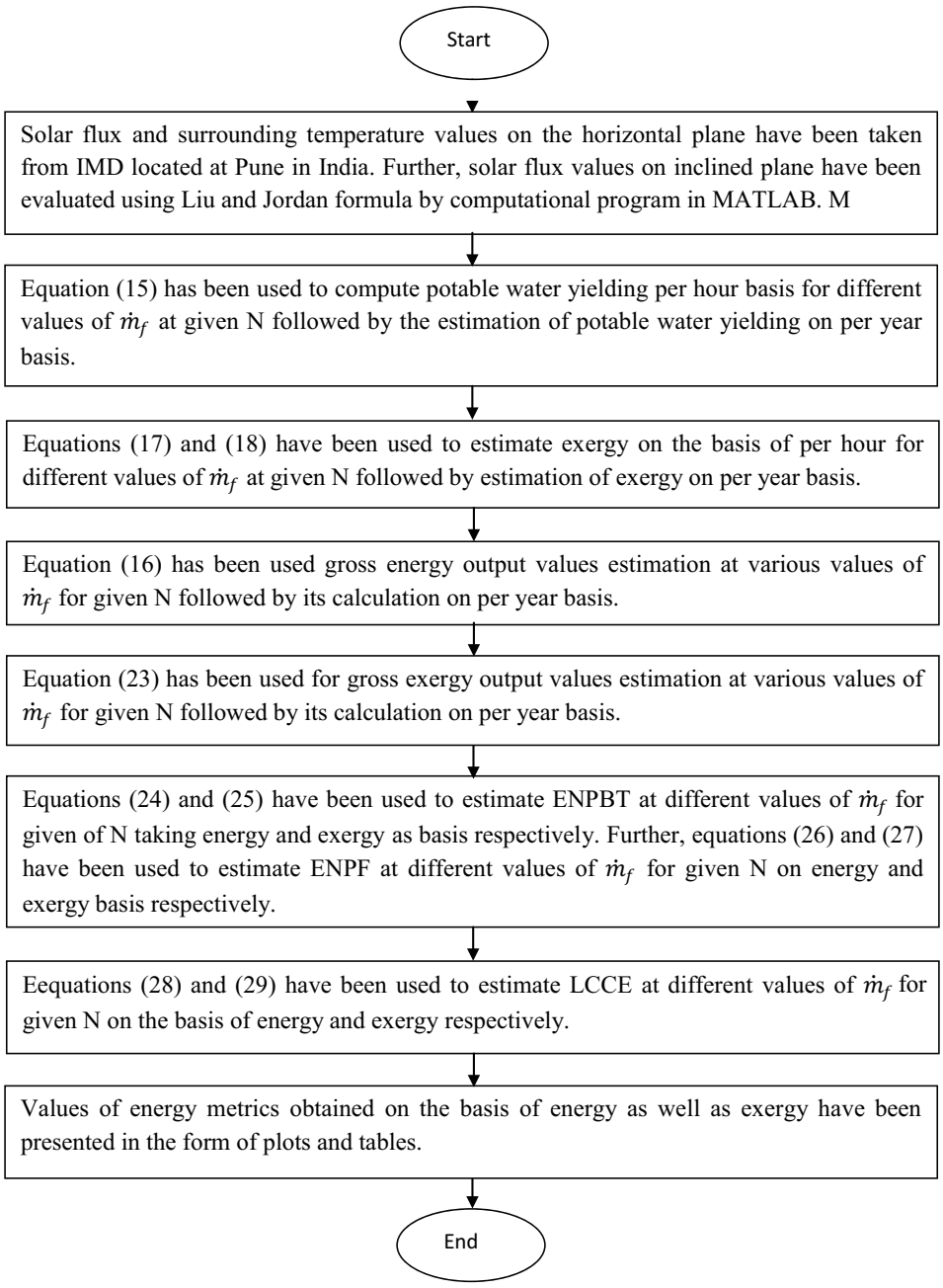

Fig. 2. Flow chart of the methodology followed for the estimation of energy metrics at different values of $\dot{m}_f$.

Step VI

The computation for energy payback time at different values of $\dot{m}_f$ for given of N has been performed with the help of Eqs. (24) and (25) taking energy and exergy as basis respectively. The computation for energy production factor at different values of $\dot{m}_f$ for given N has been carried out using Eqs. (26) and (27) on an energy and exergy basis respectively.

Step VII

The computation for life cycle conversion efficiency at different values of $\dot{m}_f$ for given N has been carried out taking the help of Eqs. (28) and (29) on the basis of energy and exergy respectively.

Flow chart of the methodology followed for the estimation of energy metrics at different values of $\dot{m}_f$ has been depicted in Fig. 2 for better understanding of the methodology.

7. Results and discussion

The required data and all relevant equations have been fed to the computational program written in MATLAB. Data on the horizontal surface has been taken from IMD Pune India. Data on the inclined surface has been

evaluated using Liu and Jordan formula with the help of MATLAB. The output of the program has been presented in Figs. 3–7 and Tables 2–7.

Table 2 represents the computation of yearly fresh water yield for NPVT-CPC-SEBDSWP at $\dot{m}_f$ = 0.02 kg/s and N = 4. The water depth has been taken as 0.14 m. Similarly, fresh water yield at other values of $\dot{m}_f$ has been evaluated and presented as Fig. 3. It is observed from Fig. 3 that the values of yield decrease as the value of $\dot{m}_f$ increases. It happens because the water flowing through tubes of the collector gets less time to absorb heat at a higher value of $\dot{m}_f$. The value of yield based on year decreases as the value of $\dot{m}_f$ increases and then it becomes almost constant because, after a certain value of $\dot{m}_f$, heat absorbed by water is very small as water flowing through tubes does not get time due to increased speed and the system behaves as working in passive mode.

Table 3 represents the computation of yearly thermal exergy for NPVT-CPC-SEBDSWP at $\dot{m}_f$ = 0.02 kg/s and N = 4. The water depth has been taken as 0.14 m. Similarly, thermal exergy at other values of $\dot{m}_f$ has been evaluated and presented as Fig. 4. It is observed from Fig. 4 that the value of thermal exergy decreases as the value of $\dot{m}_f$ increases. It happens because the water flowing through tubes of collector gets less time to absorb heat at a higher value of $\dot{m}_f$ which results in less rise in temperature of the water. The value of thermal exergy based on year decreases as the value of $\dot{m}_f$ increases and then it becomes almost constant because, after certain value of $\dot{m}_f$, heat absorbed by water is

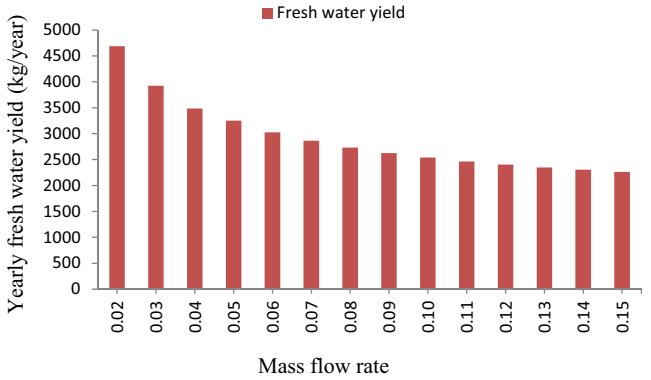

Fig. 3. Variation of yearly fresh water yield with $\dot{m}_f$ for DS type SEBWP by incorporating N equal partially covered PVT-CPCs at N = 4.

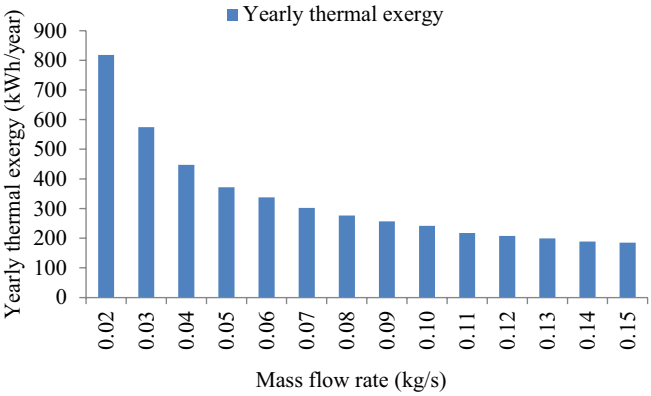

Fig. 4. Variation of yearly thermal exergy with $\dot{m}_f$ for DS type SEBWP by incorporating N equal partially covered PVT-CPCs at N = 4.

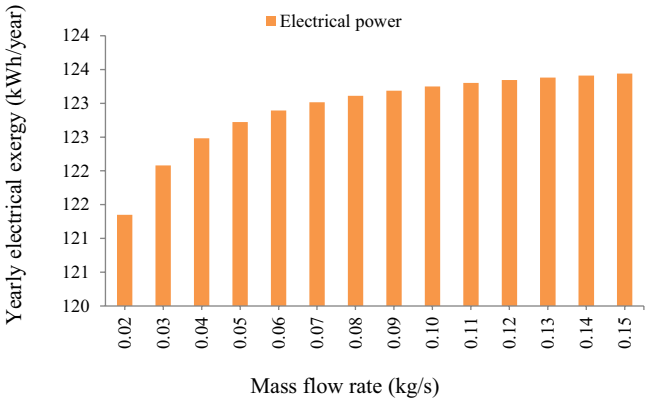

Fig. 5. Variation of yearly electrical exergy with $\dot{m}_f$ for DS type SEBWP by incorporating N equal partially covered PVT-CPCs at N = 4.

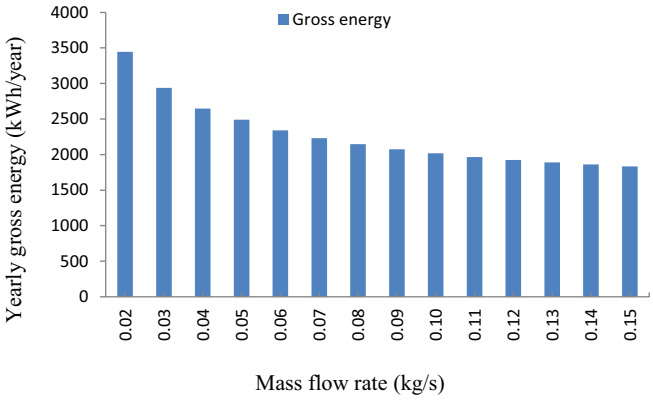

Fig. 6. Variation of yearly gross energy with $\dot{m}_f$ for DS type SEBWP by incorporating N equal partially covered PVT-CPCs at N = 4.

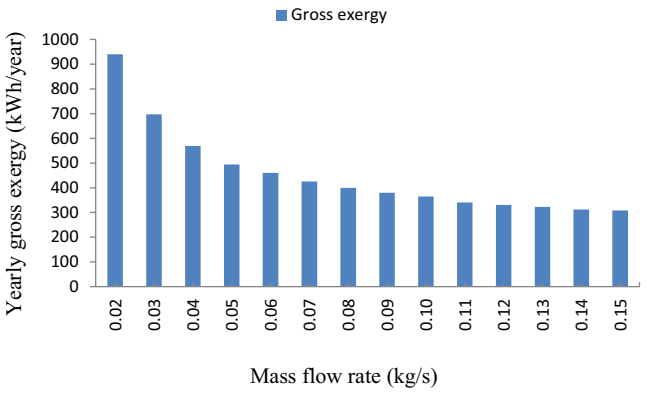

Fig. 7. Variation of yearly gross exergy with $\dot{m}_f$ for DS type SEBWP by incorporating N equal partially covered PVT-CPCs at N = 4.

Table 2
Computation of yearly fresh water yield for DS type SEBWP integrated with N equal partially covered PVT-CPCs at $\dot{m}_f$ = 0.02 kg/s, N = 4 and water depth = 0.14 m

Monthly	Daily yield	Days (Kind a)	Monthly yield (Kind a)	Daily yield	Days (Kind b)	Monthly yield (Kind b)	Daily yield	Days (Kind c)	Monthly yield (Kind c)	Daily yield	Days (Kind d)	Monthly yield (Kind d)	Gross monthly yield
Jan.	24.27	3	72.82	28.13	8	225.02	6.80	11	74.77	1.57	9	14.11	386.73
Feb.	23.23	3	69.68	22.52	4	90.06	6.87	12	82.44	1.55	9	13.91	256.09
March	25.74	5	128.69	26.65	6	159.88	11.48	12	137.76	5.57	8	44.58	470.91
April	27.79	4	111.16	27.68	7	193.79	11.64	14	162.97	9.54	5	47.72	515.64
May	27.09	4	108.36	20.72	9	186.50	13.98	12	167.75	7.95	6	47.70	510.31
June	37.02	3	111.06	20.93	4	83.72	12.24	14	171.42	4.25	6	25.48	391.67
July	22.67	2	45.34	17.63	3	52.90	12.13	10	121.26	3.56	17	60.58	280.08
Aug.	22.09	2	44.19	19.27	3	57.80	10.48	7	73.39	3.90	19	74.14	249.52
Sept.	29.23	7	204.61	25.71	3	77.14	14.24	10	142.39	5.39	10	53.87	478.02
Oct.	25.89	5	129.43	17.68	10	176.79	11.76	13	152.89	3.80	3	11.39	470.49
Nov.	23.34	6	140.01	14.75	10	147.53	5.25	12	63.00	4.30	2	8.60	359.15
Dec.	22.68	3	68.05	17.96	7	125.71	8.62	13	112.00	1.76	8	14.09	319.85
Yearly fresh water yield (kg)													4,688.47

Table 3
Computation of yearly thermal exergy for DS type SEBWP integrated with N equal partially covered PVT-CPCs at $\dot{m}_f$ = 0.02 kg/s, N = 4 and water depth = 0.14 m

Daily exergy (kWh)	Days (Kind a)	Monthly exergy (Kind a) (kWh)	Daily exergy (kWh)	Days (Kind b)	Monthly exergy (Kind b) (kWh)	Daily exergy (kWh)	Days (Kind c)	Monthly exergy (Kind c) (kWh)	Daily exergy (kWh)	Days (Kind d)	Monthly exergy (Kind d) (kWh)	Gross monthly exergy (kWh)
6.39	3	19.18	5.30	8	42.39	0.71	11	7.76	0.08	9	0.69	70.03
5.55	3	16.65	5.20	4	20.80	0.65	12	7.76	0.07	9	0.60	45.81
6.24	5	31.21	6.76	6	40.54	1.32	12	15.86	0.43	8	3.42	91.03
6.53	4	26.11	6.60	7	46.19	1.25	14	17.56	0.89	5	4.44	94.29
6.10	4	24.40	3.81	9	34.31	1.83	12	21.98	0.62	6	3.69	84.38
10.26	3	30.79	4.00	4	16.00	1.31	14	18.39	0.19	6	1.14	66.31
4.84	2	9.67	3.14	3	9.42	1.39	10	13.95	0.20	17	3.32	36.36
5.08	2	10.16	4.10	3	12.29	1.01	7	7.10	0.25	19	4.76	34.31
7.79	7	54.50	6.05	3	18.16	2.06	10	20.63	0.37	10	3.66	96.95
6.63	5	33.13	3.35	10	33.51	1.60	13	20.82	0.22	3	0.67	88.13
4.62	6	27.69	2.33	10	23.34	0.41	12	4.92	0.30	2	0.60	56.56
5.39	3	16.18	3.54	7	24.77	0.97	13	12.57	0.08	8	0.67	54.19
Yearly thermal exergy output (kWh)												818.35

Table 4
Computation of yearly electrical exergy for DS type SEBWP integrated with N equal partially covered PVT-CPCs at $\dot{m}_f$ = 0.02 kg/s, N = 4 and water depth = 0.14 m

Daily exergy (kWh)	Days (Kind a) (kWh)	Monthly exergy (Kind a) (kWh)	Daily exergy (kWh)	Days (Kind b)	Monthly exergy (Kind b) (kWh)	Daily exergy (kWh)	Days (Kind c)	Monthly exergy (Kind c) (kWh)	Daily exergy (kWh)	Days (Kind d)	Monthly exergy (Kind d) (kWh)	Gross monthly exergy (kWh)
0.646	3	1.939	0.596	8	4.769	0.309	11	3.397	0.124	9	1.114	11.219
0.616	3	1.849	0.600	4	2.401	0.299	12	3.588	0.108	9	0.968	8.807
0.597	5	2.984	0.609	6	3.652	0.339	12	4.069	0.210	8	1.677	12.381
0.566	4	2.264	0.567	7	3.967	0.301	14	4.215	0.256	5	1.279	11.724
0.523	4	2.092	0.432	9	3.890	0.317	12	3.801	0.195	6	1.173	10.956
0.670	3	2.010	0.456	4	1.825	0.284	14	3.976	0.139	6	0.833	8.644
0.495	2	0.990	0.415	3	1.244	0.302	10	3.020	0.122	17	2.077	7.331
0.510	2	1.020	0.461	3	1.382	0.262	7	1.833	0.142	19	2.689	6.924
0.561	7	3.927	0.512	3	1.536	0.337	10	3.373	0.155	10	1.547	10.383
0.552	5	2.760	0.443	10	4.435	0.342	13	4.452	0.145	3	0.434	12.081
0.546	6	3.277	0.396	10	3.959	0.211	12	2.534	0.184	2	0.368	10.138
0.588	3	1.763	0.516	7	3.611	0.337	13	4.376	0.127	8	1.013	10.763
Yearly electrical exergy output (kWh)												121.3501

very small as water flowing through tubes does not get time due to increased speed and the system behaves as working in passive mode.

Table 4 represents the computation of yearly electrical exergy for NPVT-CPC-SEBDSWP at $\dot{m}_f$ = 0.02 kg/s and N = 4. The water depth has been taken as 0.14 m. Similarly, electrical exergy at other values of $\dot{m}_f$ has been evaluated and presented as Fig. 5. It is observed from Fig. 5 that the values of electrical exergy increase as the value of $\dot{m}_f$ increases. It happens because the water flowing through tubes of collector takes away the higher amount of heat from PVT at a higher value of $\dot{m}_f$ which results in a decrease in temperature of the solar cell. Due to decreased temperature rise of the solar cell, better efficiency is obtained and hence higher electrical energy output. It is also observed that the value of electrical exergy output becomes almost constant after a certain value of $\dot{m}_f$ and then it becomes almost constant. It has been found to occur because water is not able to take away heat from PVT at a very high velocity of water because water does not have time to consume water.

Figs. 6 and 7 represent the variation of yearly energy and yearly exergy respectively with different values of $\dot{m}_f$. It is observed from Fig. 6 that the yearly gross energy decreases as the value of $\dot{m}_f$ increases due to a similar variation in yearly fresh water yield. The variation in yearly yield and yearly electrical exergy is opposite; however, the decrease in yearly fresh water yield overcome the increases in electrical energy with the increase in value of $\dot{m}_f$. Similar variation has been observed in thermal exergy.

Table 5 represents the computation of embodied energy for the proposed system and Table 6 represents the evaluation of ENPBT and ENPF on the basis of energy as well as exergy. It is observed from Table 6 that the value of ENPBT based on energy decreases as the value of $\dot{m}_f$ increases and after 0.11 kg/s the value of ENPBT based on energy becomes almost constant. It happens because of a similar variation in gross energy output. The value of ENPBT based on exergy has a similar variation.

Table 7 represents the calculation of life cycle conversion efficiency on the basis of energy as well as exergy at N = 4, water depth = 0.14 m for different values of $\dot{m}_f$ for NPVT-CPC-SEBDSWP. It is observed from Table 7 that the value of LCCE decreases as the value of $\dot{m}_f$ increases and it becomes almost constant after $\dot{m}_f$ = 0.10 kg/s. It means the optimum value of LCCE based on energy for NPVT-CPC-SEBDSWP is obtained at $\dot{m}_f$ = 0.10 kg/s. Similarly, the optimum value of LCCE based on exergy for NPVT-CPC-SEBDSWP is obtained at $\dot{m}_f$ = 0.11 kg/s.

Table 5
Embodied energy for DS type SEBWP integrated with N equal partially covered PVT-CPCs at $\dot{m}_f$ = 0.02 kg/s, N = 4 and water depth = 0.14 m

Name of component	Embodied energy (kWh)
Single slope solar still	1,737.79
CPC collector (N = 4)	3,279.42
PV (glass to glass) (N = 7)	979.55
Others	22
Total (kWh)	6,018.76

Table 6
Computation of energy payback time and ENPF for DS type SEBWP integrated with N equal partially covered PVT-CPCs at $N = 4$

Mass flow rate	Gross energy	Gross exergy	Embodied energy	ENPBT based on energy	ENPBT based on exergy	ENPF based on energy	ENPF based on exergy
kg/s	kWh	kWh	kWh	Year	Year	Per year	Per year
0.02	3,444.99	939.70	6,018.76	1.75	6.40	0.572	0.156
0.03	2,936.49	696.69	6,018.76	2.05	8.64	0.488	0.116
0.04	2,646.97	569.59	6,018.76	2.27	10.57	0.440	0.095
0.05	2,489.55	494.50	6,018.76	2.42	12.17	0.414	0.082
0.06	2,339.83	460.70	6,018.76	2.57	13.06	0.389	0.077
0.07	2,232.22	425.47	6,018.76	2.70	14.15	0.371	0.071
0.08	2,145.49	399.68	6,018.76	2.81	15.06	0.356	0.066
0.09	2,073.37	380.05	6,018.76	2.90	15.84	0.344	0.063
0.10	2,016.75	364.60	6,018.76	2.98	16.51	0.335	0.061
0.11	1,966.17	340.97	6,018.76	3.06	17.65	0.327	0.057
0.12	1,925.28	331.19	6,018.76	3.13	18.17	0.320	0.055
0.13	1,890.20	323.03	6,018.76	3.18	18.63	0.314	0.054
0.14	1,860.37	312.13	6,018.76	3.24	19.28	0.309	0.052
0.15	1,833.17	308.18	6,018.76	3.28	19.53	0.305	0.051

Table 7
Computation of LCCE for DS type SEBWP integrated with N equal partially covered PVT-CPCs at $N = 4$

Mass flow rate	Gross energy	Gross exergy	Embodied energy	Solar energy	Solar exergy	LCCE based on energy	LCCE based on exergy
kg/s	kWh	kWh	kWh	kWh	kWh	Fraction	Fraction
0.02	3,444.99	939.70	6,018.76	579,567.99	538,998.2	0.17	0.0411
0.03	2,936.49	696.69	6,018.76	579,567.99	538,998.2	0.14	0.0276
0.04	2,646.97	569.59	6,018.76	579,567.99	538,998.2	0.13	0.0205
0.05	2,489.55	494.50	6,018.76	579,567.99	538,998.2	0.12	0.0164
0.06	2,339.83	460.70	6,018.76	579,567.99	538,998.2	0.11	0.0145
0.07	2,232.22	425.47	6,018.76	579,567.99	538,998.2	0.11	0.0125
0.08	2,145.49	399.68	6,018.76	579,567.99	538,998.2	0.10	0.0111
0.09	2,073.37	380.05	6,018.76	579,567.99	538,998.2	0.10	0.0100
0.10	2,016.75	364.60	6,018.76	579,567.99	538,998.2	0.09	0.0091
0.11	1,966.17	340.97	6,018.76	579,567.99	538,998.2	0.09	0.0078
0.12	1,925.28	331.19	6,018.76	579,567.99	538,998.2	0.09	0.0073
0.13	1,890.20	323.03	6,018.76	579,567.99	538,998.2	0.09	0.0068
0.14	1,860.37	312.13	6,018.76	579,567.99	538,998.2	0.09	0.0062
0.15	1,833.17	308.18	6,018.76	579,567.99	538,998.2	0.08	0.0060

8. Conclusions

The analysis for NPVT-CPC-SEBDSWP has been done considering all four kinds of atmospheric situations to know the effect of $\dot{m}_f$ at given N on energy metrics of the system. Based on the current research study, the following conclusions have been made:

- The value of ENPBT increases with the increase in $\dot{m}_f$ and it becomes almost constant after $\dot{m}_f = 0.12$ kg/s.
- The value of ENPF increases with the increase in $\dot{m}_f$ and it becomes almost constant after $\dot{m}_f = 0.12$ kg/s.
- The value of life cycle conversion efficiency based on energy decreases with the increase in $\dot{m}_f$ and it becomes almost constant after $\dot{m}_f = 0.10$ kg/s. Similarly, the value of life cycle conversion efficiency based on exergy decreases with the increase in $\dot{m}_f$ and it becomes almost constant after $\dot{m}_f = 0.11$ kg/s.

Symbols

A_{rm} — Area of receiver covered by PV module, m^2
A_{rc} — Area of receiver covered by glass, m^2
A_{am} — Area of aperture covered by PV module, m^2
A_{ac} — Area of aperture covered by glass, m^2

A_{gE} — Area of the east glass cover, m²
A_b — Area of the basin, m²
A_{gW} — Area of the west glass cover, m²
L — Latent heat, J/kg
L_g — Thickness of glass cover, m
K_g — Thermal conductivity of glass, W/m-K
$I_b(t)$ — Beam radiation, W/m²
T_a — Ambient temperature, °C
L_i — Thickness of insulation, m
K_i — Thermal conductivity of insulation, W/m-K
α_c — Absorptivity of the solar cell
$\dot{m}_f$ — Mass flow rate of water, kg/s
τ_g — Transmissivity of the glass, fraction
C_f/C_w — Specific heat of water, J/kg-K
β_o — Temperature coefficient of efficiency, K⁻¹
L_r — Total length of receiver area, m
L_a — Total length of aperture area, m
L_{rc} — Length of receiver covered by glass
L_{rm} — Length of receiver covered by PV module
L_{ac} — Length of aperture covered by glass
L_{am} — Length of aperture covered by PV module
η_c — Solar cell efficiency
η_m — PV module efficiency
η_{cN} — Temperature-dependent electrical efficiency of solar cells of a number, N of PVT-CPC water collectors
b_r — Breath of receiver, m
b_o — Breath of aperture, m
$(\alpha\tau)_{eff}$ — Product of effective absorptivity and transmissivity
F' — Collector efficiency factor
T_c — Solar cell temperature, °C
T_p — Absorber plate temperature, °C
L_p — Thickness of absorber plate, m
K_p — Thermal conductivity of absorber plate, W/m-K
T_{fi} — Fluid temperature at collector inlet, °C
T_f — Temperature of fluid in the collector, °C
PF_1 — Penalty factor due to the glass covers of module
PF_2 — Penalty factor due to plate below the module
PF_3 — Penalty factor due to the absorption plate for the glazed portion
PF_c — Penalty factor due to the glass covers for the glazed portion
β — Packing factor of the module
η_o — Efficiency at the standard test condition
T_{foN} — Outlet water temperature at the end of Nth PVT–CPC water collector, °C
h_i — Heat transfer coefficient for space between the glazing and absorption plate, W/m²-K
h_i' — Heat transfer coefficient from the bottom of PVT to ambient, W/m²-K
h_o — Heat transfer coefficient from top of PVT to ambient, W/m²-K
U_{tca} — Overall heat transfer coefficient from cell to ambient, W/m²-K
U_{tcp} — Overall heat transfer coefficient from cell to the plate, W/m²-K
h_{pf} — Heat transfer coefficient from blackened plate to fluid, W/m²-K
U_{tpa} — Overall heat transfer coefficient from plate to ambient, W/m²-K
U_{Lm} — Overall heat transfer coefficient from module to ambient, W/m²-K
U_{Lc} — Overall heat transfer coefficient from glassing to ambient, W/m²-K
P_m — Annual power generated from the photovoltaic module, kWh
P_u — Annual power utilized by pump, kWh
ϵ — Emissivity
α' — Absorptivity
$\dot{E}x$ — Hourly exergy, W
$I(t)$ — Global solar intensity, W/m²
$I_{SE}(t)$ — Solar intensity on east glass cover, W/m²
$I_{SW}(t)$ — Solar intensity on west glass cover, W/m²
T_{giE} — Glass temperature at the inner surface of the east glass cover, °C
T_{giW} — Glass temperature at the inner surface of the west glass cover, °C
h_{rwg} — Radiative heat transfer coefficient from water to the inner surface of the glass cover, W/m²-K
h_{cwg} — Convective heat transfer coefficient from water to the inner surface of the glass cover, W/m²-K
h_{ewgE} — Evaporative heat transfer coefficient for the east side, W/m²-K
h_{ewgW} — Evaporative heat transfer coefficient for the west side, W/m²-K
M_w — Mass of water in basin, kg
$\dot{m}_{ew}$ — Mass of distillate form of double slope solar still, kg
M_{ew} — Annual yield from solar distillation system, kg
a — Clear days, blue sky
b — Hazy days, fully
c — Hazy and cloudy days, partially
d — Cloudy days, fully
$\dot{Q}_{uN}$ — The rate of useful thermal output from N identical partially (25%) covered PVT-CPC water collectors connected in series, kWh
N — Life of PVT-CPC active solar distillation system, year
I — Rate of interest, %
$G_{ex,annual}$ — Annual exergy gain, kWh
ln — Natural logarithm
DS — Double slope
T — Time, h
R — Reflectivity
SEBWP — Solar energy-based water purifier
T_s — Temperature of sun, °C
T_w — Temperature of water in the basin, °C
T_a — Ambient temperature, °C
T_{wo} — Water temperature at t = 0, °C
$\bar{T}_{cN}$ — Average solar cell temperature
E_{out} — Overall annual energy available from PVT-CPC solar distillation system, kWh
Y — Daily yield, kg
M — Monthly yield, kg
Ex — Daily exergy, kWh
Exm — Monthly exergy, kWh
N — Number of PVT-CPC water collector
E_{in} — Embodied energy, kWh

ENPF — Energy production factor, fraction
ENPBT — Energy payback time, y
LCCE — Life cycle conversion efficiency
θ — Angle of inclination of glass cover with horizontal
NPVT-CPC — N equal partially covered PVT compound parabolic concentrating collectors
FPC — Flat plate collector
PVT — Photovoltaic thermal
CPC — Compound parabolic concentrator
N' — Number of sunshine hours
r' — Daily diffuse to daily global irradiation ratio

Subscript

g — Glass
w — Water
E — East
W — West
in — Incoming
out — Outgoing
eff — Effective

References

[1] S.N. Rai, G.N. Tiwari, Single basin solar still coupled with flat plate collector, Energy Convers. Manage., 23 (1983) 145–149.
[2] S. Kumar, A. Tiwari, An experimental study of hybrid photovoltaic thermal (PV/T)-active solar still, Int. J. Energy Res., 32 (2008) 847–858.
[3] E.C. Kern, M.C. Russell, Combined Photovoltaic and Thermal Hybrid Collector Systems, Proceedings of the 13th IEEE Photovoltaic Specialists Conference, Washington, DC, USA, June 5 1958, pp. 1153–1157.
[4] G. Singh, S. Kumar, G.N. Tiwari, Design, fabrication and performance evaluation of a hybrid photovoltaic thermal (PVT) double slope active solar still, Desalination, 277 (2011) 399–406.
[5] D.B. Singh, J.K. Yadav, V.K. Dwivedi, S. Kumar, G.N. Tiwari, I.M. Al-Helal, Experimental studies of active solar still integrated with two hybrid PVT collectors, Sol. Energy, 130 (2016) 207–223.
[6] G.N. Tiwari, J.K. Yadav, D.B. Singh, I.M. Al-Helal, AM. Abdel-Ghany, Exergoeconomic and enviroeconomic analyses of partially covered photovoltaic flat plate collector active solar distillation system, Desalination, 367 (2015) 186–196.
[7] D.B. Singh, G.N. Tiwari, Enhancement in energy metrics of double slope solar still by incorporating N identical PVT collectors, Sol. Energy, 143 (2017) 142–161.
[8] D.B. Singh, Exergoeconomic and enviroeconomic analyses of N identical photovoltaic thermal integrated double slope solar still, Int. J. Exergy, 23 (2017), 347–366.
[9] D.B. Singh, N. Kumar, Harender, S. Kumar, S.K. Sharma, A. Mallick, Effect of depth of water on various efficiencies and productivity of N identical partially covered PVT collectors incorporated single slope solar distiller unit, Desal. Water Treat., 138 (2019) 99–112.
[10] D.B. Singh, Improving the performance of single slope solar still by including N identical PVT collectors, Appl. Therm. Eng., 131 (2018) 167–179.
[11] D.B. Singh, N. Kumar, S. Kumar, V.K. Dwivedi, J.K. Yadav, G.N. Tiwari, Enhancement in exergoeconomic and enviro-economic parameters for single slope solar still by incorporating N identical partially covered photovoltaic collectors, J. Sol. Energy Eng., 140 (2018) 051002 (18 pages), doi: 10.1115/1.4039632.
[12] L. Sahota, G.N. Tiwari, Exergoeconomic and enviroeconomic analyses of hybrid double slope solar still loaded with nanofluids, Energy Convers. Manage., 148 (2017) 413–430.
[13] F. Carranza, C.-D. Villa, J. Aguilara, H.A. Borbón-Nuñez, D. Sauceda, Experimental study on the potential of combining TiO_2, ZnO, and Al_2O_3 nanoparticles to improve the performance of a double-slope solar still equipped with saline water preheating, Desal. Water Treat., 216 (2021) 14–33.
[14] M.R. Kouadri, N. Chennouf, M.H. Sellami, M.N. Raache, A. Benarima, The effective behavior of ZnO and CuO during the solar desalination of brackish water in southern Algeria, Desal. Water Treat., 218 (2021) 126–134.
[15] D. Atheaya, A. Tiwari, G.N. Tiwari, I.M. Al-Helal, Analytical characteristic equation for partially covered photovoltaic thermal (PVT) compound parabolic concentrator (CPC), Sol. Energy, 111 (2015) 176–185.
[16] R. Tripathi, G.N. Tiwari, I.M. Al-Helal, Thermal modelling of N partially covered photovoltaic thermal (PVT) – compound parabolic concentrator (CPC) collectors connected in series, Sol. Energy, 123 (2016) 174–184.
[17] D.B. Singh, G.N. Tiwari, Performance analysis of basin type solar stills integrated with N identical photovoltaic thermal (PVT) compound parabolic concentrator (CPC) collectors: a comparative study, Sol. Energy, 142 (2017) 144–158.
[18] D.B. Singh, G.N. Tiwari, Exergoeconomic, enviroeconomic and productivity analyses of basin type solar stills by incorporating N identical PVT compound parabolic concentrator collectors: a comparative study, Energy Convers. Manage., 135 (2017) 129–147.
[19] D.B. Singh, G.N. Tiwari, Effect of energy matrices on life cycle cost analysis of partially covered photovoltaic compound parabolic concentrator collector active solar distillation system, Desalination, 397 (2016) 75–91.
[20] V.S. Gupta, D.B. Singh, R.K. Mishra, S.K. Sharma, G.N. Tiwari, Development of characteristic equations for PVT-CPC active solar distillation system, Desalination, 445 (2018) 266–279.
[21] V.S. Gupta, D.B. Singh, S.K. Sharma, N. Kumar, T.S. Bhatti, G.N. Tiwari, Modeling self-sustainable fully-covered photovoltaic thermal-compound parabolic concentrators connected to double slope solar distiller, Desal. Water Treat., 190 (2020) 12–27.
[22] V. Singh, D.B. Singh, N. Kumar, R. Kumar, Effect of number of collectors (N) on life cycle conversion efficiency of single slope solar desalination unit coupled with N identical partly covered compound parabolic concentrator collectors, Mater. Today:. Proc., 28 (2020) 2185–2189.
[23] D.B. Singh, G. Singh, N. Kumar, P.K. Singh, R. Kumar, Effect of mass flow rate on energy payback time of single slope solar desalination unit coupled with N identical compound parabolic concentrator collectors, Mater. Today:. Proc., 28 (4) (2020) 2551–2556.
[24] G.K. Sharma, N. Kumar., D.B. Singh, A. Mallick, Exergoeconoic analysis of single slope solar desalination unit coupled with PVT-CPCs by incorporating the effect of dissimilarity of the rate of flowing fluid mass, Mater. Today:. Proc., 28 (2020) 2364–2368.
[25] H. Prasad, P. Kumar, R.K. Yadav, A. Mallick, N. Kumar, D.B. Singh, Sensitivity analysis of N identical partially covered (50%) PVT compound parabolic concentrator collectors integrated double slope solar distiller unit, Desal. Water Treat., 153 (2019) 54–64.
[26] K. Bharti, S. Manwal, C. Kishore, R.K. Yadav, P. Tiwar, D.B. Singh, Sensitivity analysis of N alike partly covered PVT flat plate collectors integrated double slope solar distiller unit, Desal. Water Treat., 211 (2021) 45–59.
[27] D.B. Singh, Sensitivity analysis of N identical evacuated tubular collectors integrated double slope solar distiller unit by incorporating the effect of exergy, Int. J. Exergy, 34 (2021) 424–447.
[28] K. Sampathkumar, T.V. Arjunan, P. Senthilkumar, The experimental investigation of a solar still coupled with an evacuated tube collector, Energy Sources Part A, 35 (2013) 261–270.
[29] R.V. Singh, S. Kumar, M.M. Hasan, M.E. Khan, G.N. Tiwari, Performance of a solar still integrated with evacuated tube collector in natural mode, Desalination, 318 (2013) 25–33.

[30] S. Kumar, A. Dubey, G.N. Tiwari, A solar still augmented with an evacuated tube collector in forced mode, Desalination, 347 (2014) 15–24.
[31] R.K. Mishra, V. Garg, G.N. Tiwari, Thermal modeling and development of characteristic equations of evacuated tubular collector (ETC), Sol. Energy, 116 (2015) 165–176.
[32] D.B. Singh, V.K. Dwivedi, G.N. Tiwari, N. Kumar, Analytical characteristic equation of N identical evacuated tubular collectors integrated single slope solar still, Desal. Water Treat., 88 (2017) 41–51.
[33] D.B. Singh, G.N. Tiwari, Analytical characteristic equation of N identical evacuated tubular collectors integrated double slope solar still, journal of solar energy engineering: including wind energy and building energy conservation, 135 (2017) 051003 (11 pages).
[34] D.B. Singh, G.N. Tiwari, Energy, exergy and cost analyses of N identical evacuated tubular collectors integrated basin type solar stills: a comparative study, Sol. Energy, 155 (2017) 829–846.
[35] R.J. Issa, B. Chang, Performance study on evacuated tubular collector coupled solar still in West Texas climate, Int. J. Green Energy, 14 (2017) 793–800.
[36] D.B. Singh, I.M. Al-Helal, Energy metrics analysis of N identical evacuated tubular collectors integrated double slope solar still, Desalination, 432 (2018) 10–22.
[37] D.B. Singh, N. Kumar, A. Raturi, G. Bansal, A. Nirala, N. Sengar, Effect of Flow of Fluid Mass Per Unit Time on Life Cycle Conversion Efficiency of Double Slope Solar Desalination Unit Coupled with N Identical Evacuated Tubular Collectors, Lecture Notes in Mechanical Engineering, Advances in Manufacturing and Industrial Engineering, Select Proceedings of ICAPIE 2019, Springer, Singapore, 2021, pp. 393–402.
[38] S.K. Sharma, D.B. Singh, A. Mallick, S.K. Gupta, Energy metrics and efficiency analyses of double slope solar distiller unit augmented with N identical parabolic concentrator integrated evacuated tubular collectors: a comparative study, Desal. Water Treat., 195 (2020) 40–56.
[39] S.K. Sharma, A. Mallick, S.K. Gupta, N. Kumar, D.B. Singh, G.N. Tiwari, Characteristic equation development for double slope solar distiller unit augmented with N identical parabolic concentrator integrated evacuated tubular collectors, Desal. Water Treat., 187 (2020) 178–194.
[40] R.V. Patel, K. Bharti, G. Singh, R. Kumar, S. Chhabra. D.B. Singh, Solar still performance investigation by incorporating the shape of basin liner: a short review, Mater. Today:. Proc., 43 (2021) 597–604.
[41] R.V. Patel, K. Bharti, G. Singh, G. Mittal, D.B. Singh, A. Yadav, Comparative investigation of double slope solar still by incorporating different types of collectors: a mini review, Mater. Today:. Proc., 38 (2021) 300–304.
[42] R.V. Patel, G. Singh, K. Bharti, R. Kumar, D.B. Singh, A mini review on single slope solar desalination unit augmented with different types of collectors, Mater. Today:. Proc., 38 (2021) 204–210.
[43] G. Singh, D.B. Singh, S. Kumara, K. Bharti, S. Chhabra, A review of inclusion of nanofluids on the attainment of different types of solar collectors, Mater. Today:. Proc., 38 (2021) 153–159.
[44] G. Bansal, D.B. Singh, C. Kishore, V. Dogra, Effect of absorbing material on the performance of solar still: a mini review, Mater. Today:. Proc., 26 (2020) 1884–1887.
[45] P. Shankar, A. Dubey, S. Kumar, G.N. Tiwari, Production of clean water using ETC integrated solar stills: thermoenviro-economic assessment, Desal. Water Treat., 218 (2021) 106–118.
[46] S. Abdallah, M. Nasir, D. Afaneh, Performance evaluation of spherical and pyramid solar stills with chamber stepwise basin, Desal. Water Treat., 218 (2021) 119–125.
[47] D.L. Evans, Simplified method for predicting PV array output, Sol. Energy, 27 (1981) 555–560.
[48] T. Schott, Operational Temperatures of PV Modules, Proceedings of 6th PV Solar Energy Conference, London, 1985, pp. 392–396.
[49] R. Tripathi, G.N. Tiwari, Annual performance evaluation (energy and exergy) of fully covered concentrated photovoltaic thermal (PVT) water collector: an experimental validation, Sol. Energy, 146 (2017) 180–190.
[50] V.K. Dwivedi, G.N. Tiwari, Comparison of internal heat transfer coefficients in passive solar stills by different thermal models: an experimental validation, Desalination, 246 (2009) 304–318.
[51] S. Kumar, G.N. Tiwari, Estimation of convective mass transfers in solar distillation system, Sol. Energy, 57 (1996) 459–464.
[52] R.V. Dunkle, Solar Water Distillation, the Roof Type Solar Still and a Multi Effect Diffusion Still, International Developments in Heat Transfer, Proc. Int. Heat Transfer, Part V, ASME, University of Colorado, London, 1961, p. 895.
[53] R.S. Adhikari, A. Kumar, A. Kumar, Estimation of mass transfer rates in solar stills, Int. J. Energy Res., 14 (1990) 737–744.
[54] H. Zheng, X. Zhang, J. Zhang, Y. Wu, A group of improved heat and mass transfer correlations in solar stills, Energy Convers. Manage., 43 (2001) 2469–2478.
[55] J.A. Clark, The steady state performance of a solar still, Sol. Energy, 44 (1990) 43–49.
[56] H.N. Singh, G.N. Tiwari, Evaluation of cloudiness/haziness factor for composite climate, Energy, 30 (2005) 1589–1601.
[57] B.J. Huang, T.H. Lin, W.C. Hung, F.S. Sun, Performance evaluation of solar photovoltaic/thermal systems, Sol. Energy, 70 (2001) 443–448.
[58] P.K. Nag, Basic and Applied Thermodynamics, Tata McGraw-Hill, New Delhi 2004.
[59] P.I. Cooper, Digital simulation of experimental solar still data, Sol. Energy, 14 (1973) 451–456.
[60] G.N. Tiwari, R.K. Mishra, Advanced Renewable Energy Sources, Royal Society of Chemistry publishing house, UK, 2012.

Appendix-A

Expressions for various terms used in Eqs. (1) and (2) are as follows.

$$U_{\text{tca}} = \left[\frac{1}{h_o} + \frac{L_g}{K_g}\right]^{-1};\quad U_{\text{tcp}} = \left[\frac{1}{h_i} + \frac{L_g}{K_g}\right]^{-1};$$

$$h_o = 5.7 + 3.8V,\ \text{Wm}^{-2}\text{K}^{-1};\ h_i = 5.7,\ \text{Wm}^{-2}\text{K}^{-1}$$

$$U_{\text{tpa}} = \left[\frac{1}{U_{\text{tca}}} + \frac{1}{U_{\text{tcp}}}\right]^{-1} + \left[\frac{1}{h_i'} + \frac{1}{h_{\text{pf}}} + \frac{L_i}{K_i}\right]^{-1};\ h_{\text{pf}} = 100\ \text{Wm}^{-2}\text{K}^{-1}$$

$$h_i' = 2.8 + 3V',\ \text{Wm}^{-2}\text{K}^{-1}$$

$$U_{L1} = \frac{U_{\text{tcp}}U_{\text{tca}}}{U_{\text{tcp}} + U_{\text{tca}}};\ U_{L2} = U_{L1} + U_{\text{tpa}};\quad U_{\text{Lm}} = \frac{h_{\text{pf}}U_{L2}}{F'h_{\text{pf}} + U_{L2}};$$

$$U_{\text{Lc}} = \frac{h_{\text{pf}}U_{\text{tpa}}}{F'h_{\text{pf}} + U_{\text{tpa}}}$$

$$\text{PF}_1 = \frac{U_{\text{tcp}}}{U_{\text{tcp}} + U_{\text{tca}}};\ \text{PF}_2 = \frac{h_{\text{pf}}}{F'h_{\text{pf}} + U_{L2}};\ \text{PF}_c = \frac{h_{\text{pf}}}{F'h_{\text{pf}} + U_{\text{tpa}}}$$

$$(\alpha\tau)_{\text{1eff}} = \rho(\alpha_c - \eta_c)\tau_g\beta_c\frac{A_{\text{am}}}{A_{\text{rm}}};\quad (\alpha\tau)_{\text{2eff}} = \rho\alpha_p\tau_g^2(1-\beta_c)\frac{A_{\text{am}}}{A_{\text{rm}}};$$

$$(\alpha\tau)_{\text{meff}} = \left[(\alpha\tau)_{\text{1eff}} + \text{PF}_1(\alpha\tau)_{\text{2eff}}\right];\ (\alpha\tau)_{\text{ceff}} = \text{PF}_c\cdot\rho\alpha_p\tau_g\frac{A_{\text{ac}}}{A_{\text{rc}}};$$

$$A_{\mathrm{rm}} = b_r L_{\mathrm{rm}}; A_{\mathrm{am}} = b_o L_{\mathrm{am}};$$

$$A_c F_{\mathrm{Rc}} = \frac{\dot{m}_f C_f}{U_{\mathrm{Lc}}}\left[1-\exp\left(\frac{-F'U_{\mathrm{Lc}}A_c}{\dot{m}_f C_f}\right)\right];$$

$$A_m F_{\mathrm{Rm}} = \frac{\dot{m}_f C_f}{U_{\mathrm{Lm}}}\left[1-\exp\left(\frac{-F'U_{\mathrm{Lm}}A_m}{\dot{m}_f C_f}\right)\right];$$

$$\left(AF_R(\alpha\tau)\right)_1 = \left[A_c F_{\mathrm{Rc}}(\alpha\tau)_{\mathrm{ceff}} + PF_2(\alpha\tau)_{\mathrm{meff}} A_m F_{\mathrm{Rm}}\left(1-\frac{A_c F_{\mathrm{Rc}} U_{\mathrm{Lc}}}{\dot{m}_f C_f}\right)\right]$$

$$\left(AF_R U_L\right)_1 = \left[A_c F_{\mathrm{Rc}} U_{Lc} + A_m F_{\mathrm{Rm}} U_{\mathrm{Lm}} + A_m F_{\mathrm{Rm}} U_{\mathrm{Lm}}\left(1-\frac{A_c F_{\mathrm{Rc}} U_{\mathrm{Lc}}}{\dot{m}_f C_f}\right)\right]$$

$$K_k = \left(1-\frac{\left(AF_R U_L\right)_1}{\dot{m}_f C_f}\right)$$

$$\left(AF_R(\alpha\tau)\right)_{m1} = \mathrm{PF}_2(\alpha\tau)_{\mathrm{meff}} A_m F_{\mathrm{Rm}}$$

$$\left(AF_R U_L\right)_{m1} = A_m F_{\mathrm{Rm}} U_{\mathrm{Lm}}$$

$$K_m = \left(1-\frac{A_m F_{\mathrm{Rm}} U_{\mathrm{Lm}}}{\dot{m}_f C_f}\right)$$

Expressions for various terms used in Eqs. (4)–(15) are as follows.

$$a = \frac{1}{M_w C_w}\left[\begin{array}{l}\dot{m}_f C_f\left(1-K_k^N\right)+U_b A_b+\dfrac{h_{1\mathrm{wE}}\left(P-A_2\right)A_b}{2P}+\\ \dfrac{h_{1\mathrm{wW}}\left(P-B_2\right)A_b}{2P}\end{array}\right];$$

$$\overline{f}(t) = \frac{1}{M_w C_w}\left[\begin{array}{l}\left(\dfrac{\alpha'_w}{2}+h_1\alpha'_b\right)A_b\left(\overline{I}_{\mathrm{SE}}(t)+\overline{I}_{\mathrm{SW}}(t)\right)+\dfrac{\left(1-K_k^N\right)}{\left(1-K_k\right)}\\ \left(AF_R(\alpha\tau)\right)_1\overline{I}_b(t)+\left(\dfrac{\left(1-K_k^N\right)}{\left(1-K_k\right)}\left(AF_R U_L\right)_1+U_b A_b\right)T_a\\ +\left(\dfrac{h_{1\mathrm{wE}}A_1+h_{1\mathrm{wW}}B_1}{P}\right)\dfrac{A_b}{2}\end{array}\right]$$

$$A_1 = R_1 U_1 A_{\mathrm{gE}} + R_2 h_{\mathrm{EW}} A_{\mathrm{gW}}$$

$$A_2 = h_{1\mathrm{WE}} U_2 \frac{A_b}{2} + h_{\mathrm{EW}} h_{1\mathrm{wW}} \frac{A_b}{2}$$

$$P = \left(U_1 U_2 - \frac{h_{\mathrm{EW}}^2}{A_{\mathrm{gE}}} h_{1\mathrm{wW}} \frac{A_b}{2}\right) A_{\mathrm{gW}}$$

$$U_1 = \frac{h_{1\mathrm{wE}}\dfrac{A_b}{2} + h_{\mathrm{EW}}A_{\mathrm{gE}} + U_{c,\mathrm{gaE}}A_{\mathrm{gE}}}{A_{\mathrm{gW}}}$$

$$U_2 = \frac{h_{1\mathrm{wW}}\dfrac{A_b}{2} + h_{\mathrm{EW}}A_{\mathrm{gW}} + U_{c,\mathrm{gaW}}A_{\mathrm{gW}}}{A_{\mathrm{gE}}}$$

$$B_1 = \frac{\left(R_2 P + A_1 h_{\mathrm{EW}}\right)A_{\mathrm{gW}}}{U_2 A_{\mathrm{gE}}}$$

$$B_2 = \frac{\mathrm{Ph}_{1\mathrm{wW}}\dfrac{A_b}{2} + h_{\mathrm{EW}}A_{\mathrm{gW}}A_2}{U_2 A_{\mathrm{gE}}}$$

$$R_1 = \alpha'_g I_{\mathrm{SE}}(t) + U_{c,\mathrm{gaE}} T_a$$

$$R_2 = \alpha'_g I_{\mathrm{SW}}(t) + U_{c,\mathrm{gaW}} T_a$$

$$h_{\mathrm{EW}} = 0.034\times 5.67\times 10^{-8}\left[\left(T_{\mathrm{giE}}+273\right)^2+\left(T_{\mathrm{giW}}+273\right)^2\right]\left[T_{\mathrm{giE}}+T_{\mathrm{giW}}+546\right]$$

$$U_{c,\mathrm{gaE}} = \frac{\dfrac{K_g}{L_g}h_{1\mathrm{gE}}}{\dfrac{K_g}{L_g}+h_{1\mathrm{gE}}};\quad U_{c,\mathrm{gaW}} = \frac{\dfrac{K_g}{L_g}h_{1\mathrm{gW}}}{\dfrac{K_g}{L_g}+h_{1\mathrm{gW}}};$$

$$h_{1\mathrm{gE}} = 5.7+3.8V;\quad h_{1\mathrm{gW}} = 5.7+3.8V;$$

$$h_{1\mathrm{wE}} = h_{\mathrm{rwgE}} + h_{\mathrm{cwgE}} + h_{\mathrm{ewgE}}$$

$$h_{1\mathrm{wW}} = h_{\mathrm{rwgW}} + h_{\mathrm{cwgW}} + h_{\mathrm{ewgW}}$$

$$h_{e,\mathrm{wgE}} = 16.273\times 10^{-3} h_{c,\mathrm{wgE}}\left[\frac{P_w - P_{\mathrm{giE}}}{T_w - T_{\mathrm{giE}}}\right];$$

$$h_{c,\mathrm{wgE}} = 0.884\left[\left(T_w - T_{\mathrm{giE}}\right)+\frac{\left(P_w - P_{\mathrm{giE}}\right)\left(T_w+273\right)}{268.9\times 10^3 - P_w}\right]^{\frac{1}{3}};$$

$$h_{c,\mathrm{wgW}} = 0.884\left[\left(T_w - T_{\mathrm{giW}}\right)+\frac{\left(P_w - P_{\mathrm{giW}}\right)\left(T_w+273\right)}{268.9\times 10^3 - P_w}\right]^{\frac{1}{3}}$$

$$P_w = \exp\left[25.317-\frac{5{,}144}{T_w+273}\right];$$

$$P_{\mathrm{giE}} = \exp\left[25.317 - \frac{5{,}144}{T_{\mathrm{giE}} + 273}\right];$$

$$P_{\mathrm{giW}} = \exp\left[25.317 - \frac{5{,}144}{T_{\mathrm{giW}} + 273}\right];$$

$$h_{\mathrm{rwgE}} = \left(0.82 \times 5.67 \times 10^{-8}\right)\left[\left(T_w + 273\right)^2 + \left(T_{\mathrm{giE}} + 273\right)^2\right]\left[T_w + T_{\mathrm{giE}} + 546\right];$$

$$h_{\mathrm{rwgW}} = \left(0.82 \times 5.67 \times 10^{-8}\right)\left[\left(T_w + 273\right)^2 + \left(T_{\mathrm{giW}} + 273\right)^2\right]\left[T_w + T_{\mathrm{giW}} + 546\right];$$